Journal of Engineering and Technology for Industrial Applications

ISSN ONLINE: 2447-0228

ITEGAM-JETIA

Manaus, v.12 n.58, p. 602-609. March/April, 2026.
DOI: https://doi.org/10.5935/jetia. v12i58.3194

RESEARCH ARTICLE OPEN ACCESS

EXPERIMENTAL INVESTIGATION AND OPTIMIZATION ON ABRASIVE WATERJET DRILLING OF INCONEL -939 ALLOY

Praveen Jayapalan[1], Rajesh Munusamy*[2] and Sandhya Jayakumar[3]

[1, 2]Department of Mechanical Engineering, Hindustan Institute of Technology and Science, Chennai, Tamil Nadu, India - 603103.
[3]Department of Biotechnology, Hindustan Institute of Technology and Science, Chennai, Tamil Nadu, India - 603103

[1]http://orcid.org/0009-0004-5012-7357, [2]http://orcid.org/0000-0002-0419-0783, [3]http://orcid.org/0000-0001-5240-0098

Email: gg1983hebron@gmail.com, *mvrajesh1991@gmail.com, jsanbiotech@gmail.com

ARTICLE INFO

Article History
Received: December 25, 2025
Reviewed: January 9, 2026
Accepted: January 16, 2026
Published: March 31, 2026

Keywords:
Inconel-939,
Pressure,
Roughness,
Erosion,
Optimization.

ABSTRACT

Inconel 939, the nickle-based superalloy has exceptional properties that include its high thermal and mechanical behaviours. Owing to this properties Inconel 739 demand in various industries like aerospace, automobile. Machining is unavoidable to use Inconel 739 alloys. Abrasive water jet drilling (AWJD) adopted to analysis and Optimize the MRR (Material Removal Rate) and SR (Surface Roughness) by integrating the RSM (Response Surface Methodology)-CCD (Central Composite Design)-Desirability approach. The L27 Experiments conducted by adopting variation in the Pressure, Traverse Speed, Abrasive Flow Rate and Standoff gap distance. The developed model validated statistically, its suitable for further analysis. Analysis of Variations (ANOVA) illustrations the Pressure was high influential variable in the responses and optimization processes. The developed model of regression shows minimal error between predicted and actual values. Three dimensional plots and used for capture the parameters effect in the responses. Pressure was influencing the 72.7% and 78.8% on SR and MRR Respectively. Desirability approach shows the validation error less than the acceptable limits.

I. INTRODUCTION

Inconel 939 material adoptability is very high due to its unique high mechanical and thermal behaviours, when compared to other alloys such as aluminium alloys and Ti based alloys [1]. The material removed from Inconel alloys has discrete issues for conventional methods [2]. Abrasive water jet (AWJ), laser beams, exemplify unconventional machining techniques that operate through material removal mechanisms such as mechanical erosion and vaporization [3]. AWJ machining was, high pressurized water jet with abrasive particle used to cut the materials [4]. The moving Abrasive particles impacting the machined surface creates erosive wear [5]. AWJ machining can be used for many different types of machining due to its minimal barrel error.[6].

Researchers have done thorough investigations cut the material accurately and reliably so that it satisfies the needs of the product joining and assembly operations. [7]. Researchers have found crucial input parameters that significantly influence abrasive waterjet (AWJ) operations, including drilling, milling, turning, and cutting. Water jet pressure, type and size of abrasive, traversal rate, abrasive flow rate, and gap distance are essential variables [8], [9]. The suitable range of input parameters of abrasive waterjet machining can be found by optimization techniques [10]. The process needs to be optimized by suitably maximizing certain variables while keeping other variables constant [11].

Researchers have utilized many multi-objective optimization techniques, including artificial neural networks, evolutionary algorithms, the Taguchi method, and response surface methodology (RSM) to determine optimal process parameters for unconventional machining [12]. Using several such methods, multi-objective optimization strategies can improve the quality of a material. It goes beyond the problems or limits that the traditional method puts in place [13]. There is a lack of research on optimizing the inputs for abrasive waterjet drilling (AWJD) of Inconel alloys. The primary aim of this study is to regulate the most critical input parameter for the AWJD process. The cutting quality features are affected by gap distance, flow rate, travel speed, and pressure.

Desirability analysis was used to find the suitable input parameter for the different responses of Surface Roughness (SR) and Materials Removal Rate (MRR). The results obtained from the presented investigation can be effective in improving the machinability of Inconel 939 alloy and achieve higher productivity in industries.

II. MATERIALS AND METHODS

The MAXIEM 1515 type abrasive waterjet machine was used for the experiments. The drilling operation is performed as represented in Figure 1. The number of passes is restricted to one. All of these variables remain constant during the machining process. The INX-939, with a thickness of 8 mm, is utilized for AWJD. This alloy was selected as the workpiece due to its extensive utilization in many industrial applications. Tables 1 and 2 delineate the attributes and composition of INX-939.

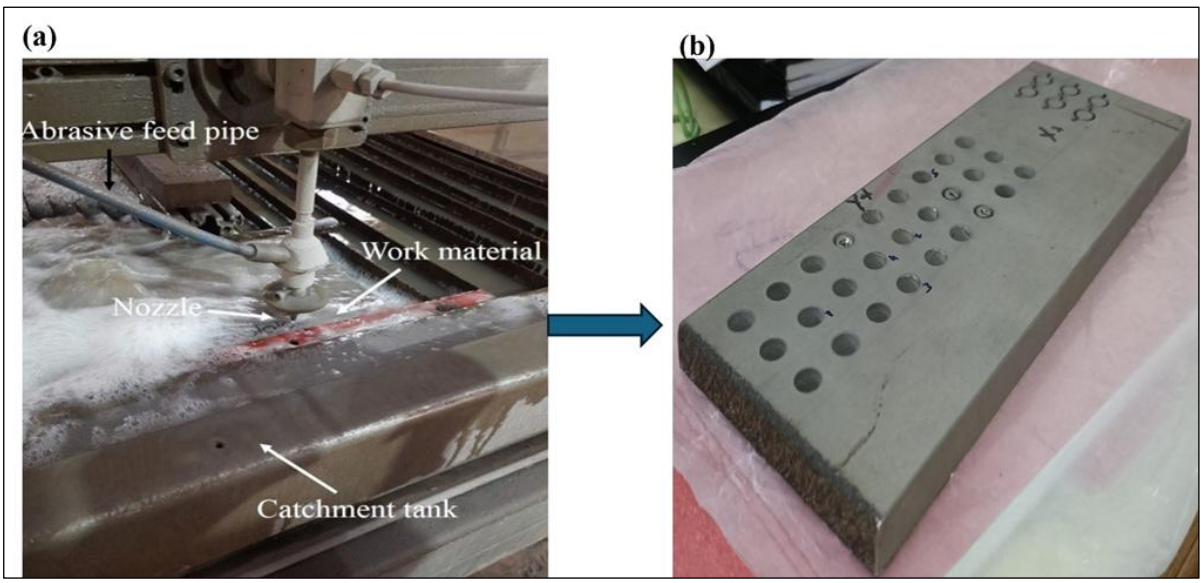

Figure 1: (a). AWJD on INX-939 cutting head, (b) Drilled Specimen.
Source: Authors, (2026).

Table 1: INX-939 Chemical Configuration (wt%)

Al	Zr	C	Cr	Co	Nb	S	P	W	B	Ti	Ta	Ni
1.99	0.09	0.14	22.38	19.25	0.99	0.001	0.002	1.97	0.011	3.65	1.45	Bal.

Source: Authors, (2026).

Table 2: Mechanical properties of INX-939.

Structure	Hardness (HRC)	Yield Strength (MPa)	Ultimate Tensile Strength (MPa)	Elastic Modulus (GPa)
Plate	38-42	850 – 950	1200 – 1400 MPa	210

Source: Authors, (2026).

This study applies several drilling conditions at 25 mm of length on target material, with an emphasis on critical output factors like undulation and circularity characteristics. During the experiment, four various levels of parameters were varied, including P, FR, TS, and SOG and their ranges were chosen based on the trial experiments are shown in Table 3 [14]. The observed reaction was analysed using the response surface methodology, and the CCD (27 trials) statistical method was employed to do rails. The trials were conducted at random [15] in order to reduce the influence of confounding variables, and two replications were obtained for each experiment. Using a contact stylus-type tester model (Surfcorder: SE3500), the top and bottom surfaces were assessed for surface roughness (SR) at the mid-depth position along the cut route. With an assessment length of 4 mm and a cut-off length of 0.8 mm, the SU was measured at a probe speed of 0.1 mm/s. For MRR, W1 is the beginning workpiece sample before machining, W2 is after machining, the density of work =8.19 g/cm3 is the cutting time (t) in minutes. as given equation (1)

$$MRR(mm^3/sec) \rightleftarrows = \frac{W_1 - W_2}{\rho \times t} \times 1000 \quad (1)$$

Table 3: The characteristics of the cutting process and the corresponding levels.

Drilling Parameters	Levels
pressure (P), MPa	120, 180, 240, 300, 360
flow rate (FR), g/min	0.45, 0.50, 0.55, 0.60, 0.65
Travel Speed (TS), mm/min	65, 73, 81, 89, 97
Standoff gap (SOG), mm	1.5, 2, 2.5, 3, 3.5

Source: Authors, (2026).

III. RESULTS AND DISCUSSIONS

III.1 RSM-CCD EVALUATION AND ANOVA ANALYSIS

This study used a central composite second-order quadratic design including a total of 27 runs. Table 4 delineates the process parameters and their respective levels within the L27 orthogonal array, along by response values for INX-929. The definitive regression models for the examined variables, specifically surface roughness and taper angle. ANOVA, executed via Design Expert software (V13), was utilized to examine the influence of process variables on machining results in the context of AWJD. The equations representing the quadratic models of the input process parameters are provided in Equations (2) and (3). Table 5 presents the results of an Analysis of Variance (ANOVA) test that evaluates the influence of process parameter values upon surface roughness (SR). The overall model has a very significant relationship as indicated by its F-statistic (F=806.88), which is associated with a very small probability ($p<0.0001$), therefore the regression model can be relied upon to predict surface roughness.

Pressure had the largest single factor effect on surface roughness (SR) as shown by its sum of squares (SS) (6.86), large F-statistic (F=2362.62) and extremely low p-value ($p<0.0001$). In addition, flow rate (SS=2.08; F=716.52) also exhibited a significant effect upon surface roughness, and then came the effects of standoff distance (SS=0.6368; F=219.22) and traverse speed (TS) (SS=0.2001; F=68.89), all three being statistically significant at $p<0.0001$. Additionally, there was very little residual error (SS=0.0639), and both the lack of fit and pure error were equal to the residual error, thus supporting the use of this model to make predictions of surface roughness. Table 6 presents the results of an ANOVA test that assesses the influences of process parameters upon material removal rate (MRR). The model had a very significant fit as demonstrated by its large F-statistic (F=1060.76), and its p-value was less than 0.0001, indicating that the model was good at making predictions of MRR.

The greatest individual effect of the various process parameters on MRR was due to pressure (P), as it had the largest sum of squares (SS) of 5253.51 and the highest F-statistic (F=3364.34). In addition, standoff gap (SOG), flow rate (FR), and traverse speed (TS) also showed a statistically significant effect on MRR as shown by their respective F-statistics of 493.35, 255.47 and 68.71, and all three were significant at $p<0.0001$. Furthermore, the residual error was minimal (SS=34.35), and the lack of fit and pure error were equal to the residual error, therefore the results demonstrate that pressure was the primary influence on MRR and that the entire set of process parameters studied had a collective influence on MRR.

$$(SR) = 4.12 + -0.6458 * P + 0.1965* FR + 0.1102 * TS -0.3553* SoG \quad (2)$$

$$(MRR) = 124.83 +17.87 * P + 6.84 * FR + 2.55 * TS +4.98* SoG \quad (3)$$

Table 4: Experimental design matrix and results for INX-929.

S.No	P	SOG	TS	FR	SR	MRR
1	300	1.5	65	0.65	3.09	128.85
2	360	1.5	97	0.65	2.88	144.22
3	360	3.5	65	0.65	3.24	152.3
4	360	1.5	65	0.45	3.51	126.05
5	360	3.5	97	0.65	3.45	157.39
6	360	3.5	65	0.45	3.88	142.63
7	360	1.5	97	0.45	3.72	132.24
8	360	2.5	81	0.55	3.59	141.31
9	360	3.5	97	0.45	4.09	147.97
10	120	1.5	65	0.65	4.08	102.78
11	240	2.5	81	0.6	3.97	129.36
12	240	2.5	73	0.55	4.08	123.41
13	240	2	81	0.55	4.05	121.32
14	240	2.5	81	0.55	4.13	124.79
15	240	2.5	81	0.55	4.13	124.79
16	240	2.5	81	0.55	4.13	124.79
17	240	2.5	89	0.55	4.19	126.25
18	240	3	81	0.55	4.25	131.16
19	120	1.5	97	0.65	4.33	107.41
20	240	2.5	81	0.5	4.33	122.11
21	120	3.5	65	0.65	4.45	114.82
22	180	2.5	81	0.55	4.46	116.15
23	120	3.5	97	0.65	4.73	119.06
24	120	1.5	65	0.45	4.84	94.1
25	120	3.5	65	0.45	5.12	106.19
26	120	1.5	97	0.45	5.07	98.47
27	120	3.5	97	0.45	5.38	110.57

Source: Authors, (2026).

Table 5: ANOVA analysis and effects of process parameter on SR.

Source	SS	D0f	MS	F-value	p-value
Model	9.38	4	2.34	806.88	< 0.0001
PRESSURE	6.86	1	6.86	2362.62	< 0.0001
Standoff distance	0.6368	1	0.6368	219.22	< 0.0001
TS	0.2001	1	0.2001	68.89	< 0.0001
flow rate	2.08	1	2.08	716.52	< 0.0001
Residual	0.0639	22	0.0029		
Lack of Fit	0.0639	20	0.0032		
Pure Error	0	2	0		
Cor Total	9.44	26			

Source: Authors, (2026).

Table 6. ANOVA analysis and effects of process parameter on MRR

Source	SS	dof	MS	F-value	p-value
Model	6625.64	4	1656.41	1060.76	< 0.0001
P	5253.51	1	5253.51	3364.34	< 0.0001
SOG	770.38	1	770.38	493.35	< 0.0001
TS	107.3	1	107.3	68.71	< 0.0001
FR	398.93	1	398.93	255.47	< 0.0001
Residual	34.35	22	1.56		
Lack of Fit	34.35	20	1.72		
Pure Error	0	2	0		
Cor Total	6659.99	26			

Source: Authors, (2026).

The tight clustering of data points in figure 2 (a), which is a scatter-plot of actual vs. predicted values on a normalized range of 2.5 to 5.5, indicates that there was good agreement between actual and predicted values. On average, most of the predictions were within ±0.2 units of their respective actual values, with little spread throughout the range. Therefore, it can be concluded that the model had relatively low prediction error, and therefore a high level of model fidelity in the normalized domain. In addition, figure 2 (b) shows the predicted vs. actual values on an expanded range of 90 to 160. Like figure 2 (a), the scatter-plot in figure 2 (b) also demonstrates similar alignment to the diagonal, and thus has similar predictive performance. Additionally, the majority of data points are less than ±5 units from the ideal prediction line, with the greatest density of data points found at values between 110 to 140. Overall, the proximity of each figure's data points to the ideal prediction line, regardless of the output range, further supports the overall robustness of the model for predicting values across different scales.

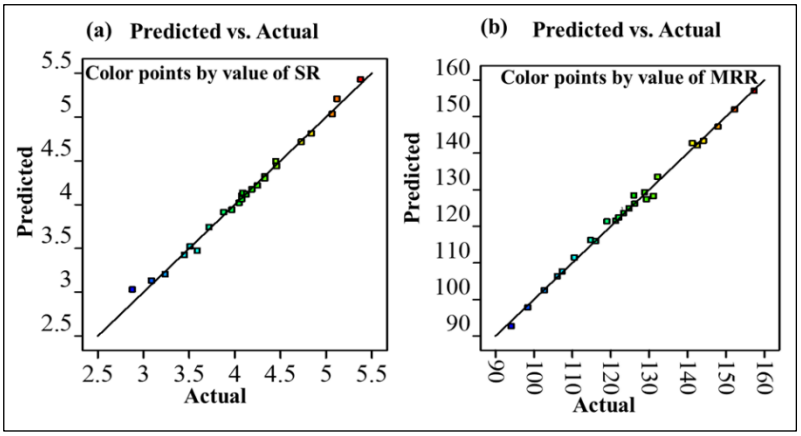

Figure 2: Pred vs Actual plot (a) SR and (b) MRR.
Source: Authors, (2026).

III.2 RSM ANALYSIS OF SR

Pressure and standoff distance in relation to surface roughness are shown in figure 3(a). In general, as pressure is increased (from 120 to 360 MPa), there will be a decrease in SR and this is especially true for low standoff distances (i.e., 1.5-2.0 mm) and when viewed on a surface plot, it shows the surface to appear smoother. Pressure and traverse speed (TS) interaction effects on SR are presented in figure 3(b). Once again, it can be seen that pressure increases coupled with moderate traverse speeds (approximately 80 mm/min) produce lower SR values, indicating that a range of optimal processing parameters exists. As presented in figure 3(c), the correlation of pressure and flow rate indicates that increased pressure and reduced flow rates (approximately 0.45-0.50 kg/min) contribute to minimizing SR. All three figures indicate that the model's predictions of SR are accurate based upon the placement of red data points along the surface contours and that pressure is the most influential parameter in achieving better surface finishes.

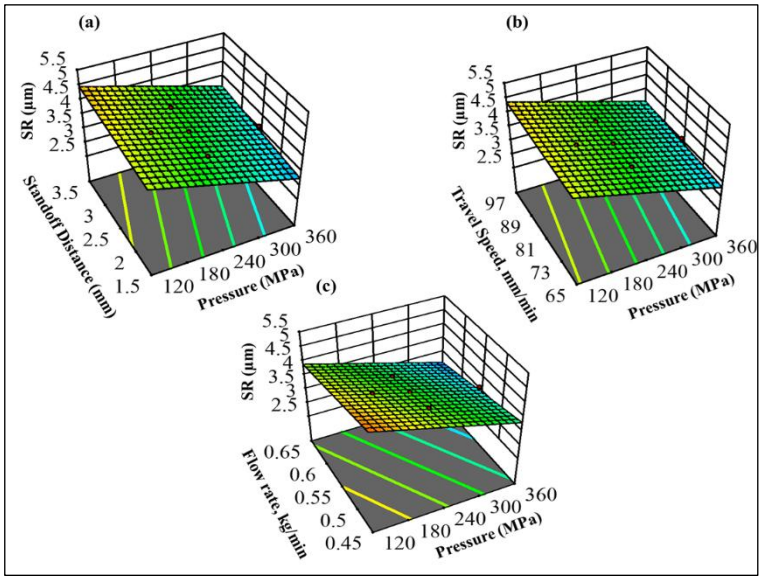

Figure 3: (a,b & c) 3D Undulation plots for SR.
Source: Authors, (2026).

III.3 RSM ANALYSIS OF MRR

As shown in figure 4(a), it is clear how the pressure and the distance from the workpiece surface affects the material removal rate (MRR) since it can be seen in this surface plot that an increase in pressure from 120 MPa up to 360 MPa has a very significant impact on MRR; especially when the distance from the workpiece surface is low (i.e., 1.5-2.0 mm). For example, MRR almost reaches its highest point of approximately 160 mm³/sec at these lower distances from the workpiece surface. In addition, as indicated by the interaction plot in figure 4(b) between pressure and traverse speed (TS), it can be observed that as the pressure is increased so does MRR. Additionally, the MRR is at an optimal level for moderate TS (i.e., 80 mm/min); after which it will plateau. Finally, figure 4(c) depicts the effects of pressure and flow rate on MRR, and indicates that high pressure combined with low flow rate (i.e., 0.45-0.50 kg/min) produces the highest MRR. In all three plots, the red data points are close to the surface contours, thus verifying the accuracy of the model and demonstrating the effect of pressure as the key factor in achieving the maximum MRR

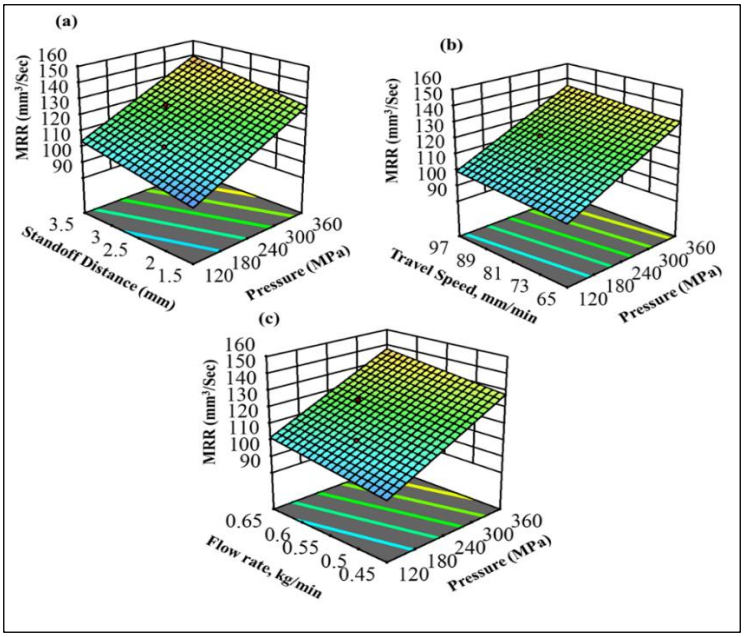

Figure 4: (a,b & c) 3D Undulation plots for MRR.
Source: Authors, (2026).

III.4 DESIRABILITY ANALYSIS

In figure 5 (a) we have a perturbation plot that illustrates how sensitive the entire desirability function is to changes in each process variable (pressure A, standoff B, traverse C, flow D) in coded units. The steep slope of the green line representing pressure suggests it has a large impact on what the best optimized solution is. The flat lines of the other variables indicate less sensitivity in this region. In figure 5(b) we have a desirability bar chart displaying the individual and collective desirability scores of the optimal solution (solution 1 of 100) for the process parameters of interest (pressure, standoff, traverse, flow). Each of the four process parameters of interest; pressure, standoff, traverse, and flow all reach the highest desirability of 1.0, which is the ideal setting for each variable.

The response desirability values are; 0.870951 for surface roughness, 0.913342 for material removal rate (MRR), and 0.891894 for the combined objective, as they represent an acceptable balance of surface finish with machining efficiency. Figure 5(c) presents the optimal values for the process parameters and associated response values. This set of conditions includes; maximum pressure (360 MPa), maximum standoff (3.5 mm), minimum traverse (65 mm/min), and maximum flow (0.65 kg/min). With these conditions the predicted surface roughness is 3.20262 microns and the MRR is 151.905 mm^3/sec, both of which fall in the desired operating range. This confirms the effectiveness of the multi-objective optimization method in finding a robust process window that will optimize both surface finish and material removal efficiency [16-18].

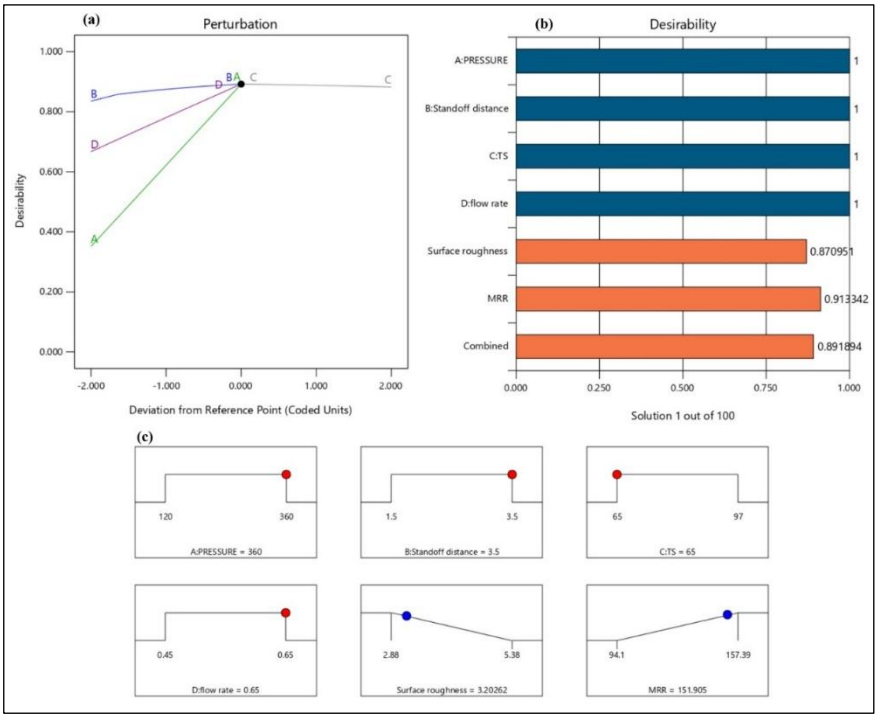

Figure 5: (a) Perturbation, (b) Bar & (c) Ramp.
Source: Authors, (2026).

Table 7: Desirability results.

Number	P	SOG	TS	FR	SR	MRR	Desirability
1	360	3.5	65	0.65	3.203	151.905	0.892
2	359.999	3.499	66.779	0.65	3.215	152.179	0.892
3	360	3.483	65.786	0.65	3.205	151.915	0.892
4	360	3.5	66.952	0.65	3.216	152.216	0.892
5	360	3.5	67.27	0.65	3.218	152.267	0.891
6	360	3.499	68.095	0.65	3.224	152.393	0.891
7	360	3.446	67.045	0.65	3.206	151.863	0.891
8	359.816	3.5	68.363	0.65	3.227	152.413	0.891
9	359.957	3.5	69.6	0.65	3.235	152.629	0.891
10	360	3.482	70.697	0.65	3.238	152.692	0.891
11	359.999	3.499	71.687	0.65	3.249	152.968	0.891
12	359.892	3.5	71.119	0.65	3.245	152.865	0.89
13	359.917	3.5	71.562	0.65	3.248	152.939	0.89
14	359.609	3.5	70.319	0.65	3.241	152.695	0.89
15	360	3.299	65.884	0.65	3.169	150.67	0.889
16	360	3.5	65.004	0.647	3.212	151.778	0.889
17	360	3.396	74.125	0.65	3.245	152.652	0.889
18	359.987	3.459	76.954	0.65	3.277	153.526	0.889
19	360	3.274	65	0.65	3.159	150.355	0.889
20	360	3.5	80.67	0.65	3.311	154.403	0.888
21	359.741	3.5	79.091	0.65	3.301	154.113	0.888
22	360	3.499	81.135	0.65	3.314	154.473	0.888
23	360	3.5	80.221	0.65	3.308	154.319	0.888
24	359.999	3.221	66.465	0.65	3.158	150.234	0.888
25	360	3.5	82.72	0.65	3.325	154.728	0.887
26	360	3.165	65.002	0.65	3.137	149.614	0.887
27	359.999	3.499	83.822	0.65	3.332	154.898	0.887
28	360	3.322	79.343	0.65	3.266	152.973	0.887
29	359.578	3.201	65.001	0.65	3.146	149.801	0.887
30	359.997	3.5	84.457	0.65	3.337	155	0.887

Source: Authors, (2026).

III.5 CONFIRMATION TEST

The experimental validation of the optimized process parameters for maximizing the Material Removal Rate (MRR) and minimizing the Surface Roughness (SR) are shown in Table 8. The initial working parameters of 200 MPa pressure, 0.4 kg/min flow rate, 60 mm/min traverse speed and 2 mm standoff gap resulted in a SR of 4.3 microns and an MRR of 149.21 mm^3/s. Following the completion of the multi-objective optimization process, the optimized parameters of 360 MPa pressure, 0.65 kg/min flow rate, 65 mm/min traverse speed and 3.5 mm standoff gap were experimentally verified. Under the above conditions the actual measured SR was 2.84 microns and the MRR was 153.57 mm^3/s; which is very similar to the predicted values of 3.2 microns and 151.9 mm^3/s. Therefore, there has been a 12.67% improvement in SR and a 1.08% increase in MRR over the base case. The close correlation between the predicted and experimental results indicate that the optimization model is reliable and applicable for optimizing machining performance [19], [20].

Table 8. Experimental Validation.

Confirmation	Parameters Range	SR	MRR
Initial condition	P = 200 Mpa, FR = 0.4 Kg/min, TS= 60 mm/min, SOG= 2 mm	4.3	149.21
Predicted	P = 360 Mpa, FR = 0.65 Kg/min, TS= 65 mm/min, SOG= 3.5 mm	3.2	151.90
Actual	P = 360 Mpa, FR = 0.65 Kg/min, TS= 65 mm/min, SOG= 3.5 mm	2.84	153.57
Improvement (%)		12.67	1.08

Source: Authors, (2026).

IV. CONCLUSIONS

The study demonstrated the effectiveness of process parameter optimization for AWJD machining process for INX -939 through systematic evaluation of the key process parameters like pressure, flow rate, travel speed and standoff gap. The experimental investigation employed the response surface technique to improve the input settings of abrasive water jet drilling (AWJD) process for the superalloy. The objective was to reduce surface roughness and increase MRR, two significant variables that influence the precision and quality of the machined products. The research showed that the MRR and surface roughness may be greatly enhanced by modifying the input parameters. During the investigation, the following particular observations were made:

• The ANOVA results show that both surface roughness (SR) and material removal rate (MRR) are significantly influenced by the factors included in the model, and that the models are very reliable given the very high F-values and p-values less than 0.0001 for all parameters evaluated. Pressure is found to be the most influential parameter affecting both surface roughness and material removal rate. However, flow rate, standoff distance, and traverse speed also have a significant impact on response variables. Low pure error and minimal residual error support the validity of the models used to predict machining performance. As a result, the ANOVA provides evidence that the selected process parameters affect the machining performance through a quantifiable mechanism. It further establishes pressure as a primary variable controlling machining performance and supports the robustness of the models for use in both predictive and optimization efforts.

• An analysis of the desirability function indicates that the optimal process parameter setting yields a balance of performance improvements for multiple objective functions. Given that all of the process parameters reach their optimal desirability (i.e., value = 1.0), the model determines that pressure, standoff distance, traverse speed, and flow rate are all at their optimal operating points. The desirability-based technique yields a total desirability of 0.891894, corroborated by individual desirability scores of 0.870951 for surface roughness and 0.913342 for material removal rate. So, the desirability-based optimization technique works well to lower surface roughness and raise the efficiency of material removal. This shows that the desirability-based approach can improve machining quality and productivity.

• Validation experimental trials depicted that the modified process parameters lead to greater machining performance. When we looked at the optimized process parameters and the original machining parameters side by side, we saw that the surface roughness went down by 12.67% and the rate of material removal went up by 1.08%. The fact that the projected values were close to the measured values during the validation experiments shows that the multi-objective optimization model is reliable and might be used to improve machining performance.

V. AUTHOR'S CONTRIBUTION

Conceptualization: Praveen Jayapalan, Rajesh Munusamy and Sandhya Jayakumar.
Methodology: Praveen Jayapalan, Rajesh Munusamy and Sandhya Jayakumar.
Investigation: Praveen Jayapalan, Rajesh Munusamy and Sandhya Jayakumar.
Discussion of results: Praveen Jayapalan, Rajesh Munusamy and Sandhya Jayakumar.
Writing – Original Draft: Praveen Jayapalan, Rajesh Munusamy and Sandhya Jayakumar.
Writing – Review and Editing: Rajesh Munusamy and Sandhya Jayakumar.
Resources: Praveen Jayapalan, Rajesh Munusamy and Sandhya Jayakumar.
Supervision: Rajesh Munusamy and Sandhya Jayakumar.
Approval of the final text: Praveen Jayapalan, Rajesh Munusamy and Sandhya Jayakumar.

VI. ACKNOWLEDGMENTS

This work was supported by the Hindustan Institute of Technology and Science, Padur, Chennai-603103 [SEED/CRC/HITS/2022-23-008]

VII. REFERENCES

[1] M. A. Iqbal, K. Skotnicová, A. Shafiq, and T. N. Sindhu, “Inconel alloys: A comprehensive review of properties and advanced manufacturing techniques,” International Journal of Thermofluids, vol. 29, p. 101394, Sep. 2025, doi: 10.1016/j.ijft.2025.101394.

[2] A. F. V. Pedroso et al., “An In-Depth Exploration of Unconventional Machining Techniques for INCONEL® Alloys,” Materials, vol. 17, no. 5, p. 1197, Mar. 2024, doi: 10.3390/ma17051197.

[3] P. Singh, A. Pramanik, A. K. Basak, C. Prakash, and V. Mishra, “Developments of non-conventional drilling methods—a review,” The International Journal of Advanced Manufacturing Technology, vol. 106, no. 5–6, pp. 2133–2166, Jan. 2020, doi: 10.1007/s00170-019-04749-0.

[4] X. Xue, O. Salenko, H. Habuzian, and A. Havrushkevych, “A Review of Abrasive Water Jet Cutting Technology for Composite Materials,” Mechanics and Advanced Technologies, vol. 9, no. 3(106), pp. 372–385, Sep. 2025, doi: 10.20535/2521-1943.2025.9.3(106).315941.

[5] N. Yuvaraj and M. Pradeep Kumar, “Study and evaluation of abrasive water jet cutting performance on AA5083-H32 aluminum alloy by varying the jet impingement angles with different abrasive mesh sizes,” Machining Science and Technology, vol. 21, no. 3, pp. 385–415, Jul. 2017, doi: 10.1080/10910344.2017.1283958.

[6] F. Kartal and A. Kaptan, “Comprehensive and essential review of advanced researches abrasive waterjet machining,” International Advanced Researches and Engineering Journal, vol. 9, no. 1, pp. 50–69, Apr. 2025, doi: 10.35860/iarej.1582470.

[7] M. Li, M. Huang, Y. Chen, W. Kai, and X. Yang, “Experimental study on hole characteristics and surface integrity following abrasive waterjet drilling of Ti6Al4V/CFRP hybrid stacks,” The International Journal of Advanced Manufacturing Technology, vol. 104, no. 9–12, pp. 4779–4789, Oct. 2019, doi: 10.1007/s00170-019-04334-5.

[8] K. Balaji, M. Siva Kumar, and N. Yuvaraj, “Multi objective taguchi–grey relational analysis and krill herd algorithm approaches to investigate the parametric optimization in abrasive water jet drilling of stainless steel,” Appl Soft Comput, vol. 102, p. 107075, Apr. 2021, doi: 10.1016/j.asoc.2020.107075.

[9] Y. Natarajan, P. K. Murugesan, M. Mohan, and S. A. Liyakath Ali Khan, “Abrasive Water Jet Machining process: A state of art of review,” J Manuf Process, vol. 49, pp. 271–322, Jan. 2020, doi: 10.1016/j.jmapro.2019.11.030.

[10] Y. Natarajan, P. K. Murugesan, M. Mohan, and S. A. Liyakath Ali Khan, “Abrasive Water Jet Machining process: A state of art of review,” J Manuf Process, vol. 49, pp. 271–322, Jan. 2020, doi: 10.1016/j.jmapro.2019.11.030.

[11] M. Santhanakumar, R. Vijayakumar,R. Adalarasan, and M. Rajesh, “An in-depth investigation on kerf angle in pierced hole on inconel-625 superalloy using abrasive waterjet cutting process,” Surface Review and Letters, vol. 31, no. 12, Dec. 2024, doi: 10.1142/S0218625X24500999.

[12] R. K. Thakur and K. K. Singh, “An investigation into the impact of graphene nanoplatelets reinforced with glass fiber reinforced polymer composite on the hole quality using abrasive water jet drilling,” Polym Compos, vol. 43, no. 10, pp. 7007–7027, Oct. 2022, doi: 10.1002/pc.26762.

[13] S. R. N., D. Tirumala, R. Gajjela, and R. Das, “ANN and RSM approach for modelling and multi objective optimization of abrasive water jet machining process,” Decision Science Letters, pp. 535–548, 2018, doi: 10.5267/j.dsl.2017.11.003.

[14] N. Srirangarajalu, R. Vijayakumar, and M. Rajesh, “Multi performance investigation of Inconel-625 by abrasive aqua jet cutting,” Materials and Manufacturing Processes, vol. 37, no. 12, pp. 1393–1404, Sep. 2022, doi: 10.1080/10426914.2021.2006225.

[15] Y. Natarajan, P. K. Murugesan, M. Mohan, and S. A. Liyakath Ali Khan, “Abrasive Water Jet Machining process: A state of art of review,” J Manuf Process, vol. 49, pp. 271–322, Jan. 2020, doi: 10.1016/j.jmapro.2019.11.030.

[16] R. Vijayakumar, N. Srirangarajalu, M. Santhanakumar, N. E. E. Paul, and M. Rajesh, “Investigation of Abrasive Aqua Jet Hole Making (AAJHM) parameters using desirability analysis on Inconel-625 space alloy,” J Manuf Process, vol. 92, pp. 311–328, Apr. 2023, doi: 10.1016/j.jmapro.2023.03.008.

[17] R. Pahuja and R. M., “Abrasive water jet machining of Titanium (Ti6Al4V)–CFRP stacks – A semi-analytical modeling approach in the prediction of kerf geometry,” J Manuf Process, vol. 39, pp. 327–337, Mar. 2019, doi: 10.1016/j.jmapro.2019.01.041.

[18] M. Li, M. Huang, Y. Chen, P. Gong, and X. Yang, “Effects of processing parameters on kerf characteristics and surface integrity following abrasive waterjet slotting of Ti6Al4V/CFRP stacks,” J Manuf Process, vol. 42, pp. 82–95, Jun. 2019, doi: 10.1016/j.jmapro.2019.04.024.

[19] R. Vijayakumar, N. Srirangarajalu, M. Santhanakumar, and R. Adalarasan, “Investigation in µ-WEDM of Inconel 625 superalloy using RSM-CCD technique,” Materials and Manufacturing Processes, vol. 38, no. 4, pp. 449–460, Mar. 2023, doi: 10.1080/10426914.2022.2116035.

[20] M. Santhanakumar, R. Adalarasan, and M. Rajmohan, “Experimental Modelling and Analysis in Abrasive Waterjet Cutting of Ceramic Tiles Using Grey-Based Response Surface Methodology,” Arab J Sci Eng, vol. 40, no. 11, pp. 3299–3311, Nov. 2015, doi: 10.1007/s13369-015-1775-x.